Ailanthone inhibits cell growth and migration of cisplatin resistant bladder cancer cells through down-regulation of Nrf2, YAP, and c-Myc expression

Ailanthone inhibits cell growth and migration of cisplatin-resistant bladder cancer cells through down-regulation of Nrf2, YAP and c-Myc expression.

Martina Daga[a, 1], Stefania Pizzimenti[a, 1,*], Chiara Dianzani[b], Marie Angele Cucci[a], Roberta Cavalli[b], Margherita Grattarola[a], Benedetta Ferrara [b], Francesco Trotta[c, 2] and Giuseppina Barrera[a, 2]

[a] Department of Clinical and Biological Science, University of Turin, Corso Raffaello 30, 10125 Torino, (Italy)

[b] Department of Drug Science and Technology, University of Turin, Via Pietro Giuria 9, 10125 Turin, Italy

[c] Department of Chemistry, University of Turin, Via Pietro Giuria 7, 10125 Turin, Italy

[1]Martina Daga and Stefania Pizzimenti contributed equally to this work.

*Corresponding Author
Stefania Pizzimenti, Department of Clinical and Biological Science, University of Turin, Corso Raffaello 30, 10125 Torino, (Italy)
Tel: +39-011-6707792; Fax: +39-011-6707753
Mail: stefania.pizzimenti@unito.it

[2] Co-last authors.

WORD COUNT: 4.972

Abstract

Background: Ailanthone (Aila) is a natural active compound isolated from the Ailanthus altissima, which has been shown to possess an "in vitro" growth-inhibitory effect against several cancer cell lines. Advanced bladder cancer is a common disease characterized by a frequent onset of resistance to cisplatin-based therapy. The cisplatin (CDDP) resistance is accompanied by an increase in Nrf2 protein expression which contributes to conferring resistance. Recently, we demonstrated a cross-talk between Nrf2 and YAP. YAP has also been demonstrated to play an important role in chemoresistance of bladder cancer.

Purpose: We analyzed the antitumor effect of Aila in sensitive and CDDP-resistant bladder cancer cells and the molecular mechanisms involved in Aila activity.

Study design: Sensitive and CDDP-resistant 253J B-V and 253J bladder cancer cells, and intrinsically CDDP-resistant T24 bladder cancer cells were used. Cells were treated with diverse concentrations of Aila and proliferation, cell cycle, apoptosis and gene expressions were determined.

Methods: Aila toxicity and proliferation were determined by MTT and colony forming methods, respectively. Cell cycle was determined at cytofluorimeter by PI staining method. Apoptosis was detected using Annexin V and PI double staining followed by quantitative flow cytometry. Expressions of Nrf2, Yap, c-Myc, and house-keeping genes were determined by western blot with specific antibodies. Cell migration was detected by wound healing and Boyden chamber analysis.

Results: Aila inhibited growth of sensitive and CDDP-resistant bladder cancer cells with the same effectiveness, and reduced cell migration with higher effectiveness in CDDP resistant cells. Interestingly, Aila strongly reduced Nrf2 expression in all cell lines. Cell cycle analysis revealed an accumulation of Aila-treated cells in G0/G1 phase. Moreover, Aila significantly reduced YAP and c-Myc protein expression. The random and the oriented migration were strongly inhibited by Aila treatment, in particular in CDDP-resistant cells.

Conclusions: Aila, inhibited proliferation and invasiveness of bladder cancer cells. Its high effectiveness in CDDP resistant cells could be related to the inhibition of Nrf2 , YAP and c-Myc expressions. Aila could represent a new tool to overcome CDDP resistance in bladder cancer.

Keywords: Ailanthone; bladder cancer; CDDP-resistance; Nrf2; Yap; c-Myc.

Abbreviation: Aila, Ailanthone; CDDP, Cisplatin; Nrf2, NF-E2-related factor 2; YAP, yes-associated protein; MTT, 3-(4,5-Dimethylthiazol-2-yl)-2,5-diphenyltetrazolium bromide; Keap1, Kelch-like ECH-associated protein 1; ARE, antioxidant response element; EpRE, electrophile response element; RPMI 1640, Roswell Park Memorial Institute medium; FBS, fetal bovine serum; EDTA: Ethylenediaminetetraacetic acid; SDS, sodium dodecyl sulfate; TBS: tris-buffered saline; GAPDH, glyceraldehyde 3 phosphate dehydrogenase; GSTA4, Glutathione S-transferase A4; PI, propidium iodide, FITC, fluorescein isothiocyanate;

Introduction

Ailanthone (Aila) [(1β,11β,12α)-11,20-Epoxy-1,11,12-trihydroxypicrasa-3,13(21)-diene-2,16-dione] is a natural active compound isolated from the plant Ailanthus altissima (Bray et al., 1987). Aila has a wide spectrum of biological activities, it is traditionally used to treat ascariasis, diarrhoea, spermatorrhoea, bleeding and gastrointestinal diseases, and it has been found to have anti-inflammatory activity (Kim et al., 2015). Aila has been shown to possess an "in vitro" growth-inhibitory effect against several cancer cell lines (Wang R. et al., 2016), but the mechanisms involved in the antiproliferative activity of Aila are not completely elucidated and they seem to be related to the cancer cell type. Indeed, in some cell models Aila induced G0/G1-phase cell cycle arrest, and triggered DNA damage and apoptosis pathway (Zhuo et al., 2015), in others, Aila induced G2/M phase cell cycle arrest and an apoptosis through downregulation of Bcl2 and upregulation of Bax (Chen Y et al., 2017). Ni et al. (2017) found that Aila inhibited the growth of several lung cancer cells through repression of DNA replication via RPA1 down regulation. He et al. (2016) demonstrated that Aila was a potent inhibitor of androgen receptor and it was able to overcome resistance in castration-resistant cancer cells through the binding with the co-chaperone p23 protein.

Urothelial carcinoma of the bladder is a common malignancy in men. At the initial diagnosis, about 30% of tumors have already infiltrated the bladder muscle wall and are classified as muscle-invasive bladder cancers. Muscle-invasive bladder cancer is associated with poor prognosis. Standard of care for muscle-invasive bladder cancer is cystectomy combined with platinum-based chemotherapy regimens (Madersbacher et al., 2003). The clinical benefit of cisplatin-based chemotherapy is limited and the majority of the patients eventually develop cisplatin-resistant disease (Shah et al., 2011). Thus, the identification of novel agents able to overcome this resistant disease is an urgent and unmet need.

In bladder cancer cells, we previously demonstrated that the CDDP resistance was accompanied by an increase in Nrf2 (NF-E2-related factor 2) protein expressions which contributes to conferring CDDP resistance (Ciamporcero et al., 2018). The transcription factor Nrf2 is the master regulator of antioxidant and cytoprotective genes (Rojo de la Vega et al., 2018). It is present in the cytoplasm bound to Keap1 (Kelch-like ECH-associated protein 1) which, by forming a complex with Cul3 and Rbx1, and this E3 ubiquitin ligase complex, is able to ubiquitinate Nrf2, resulting in Nrf2 proteasomal degradation. In response to an increase of oxidative stress, the cysteine residues of Keap1 become oxidized, resulting in a conformational change of the Keap1–Nrf2 complex which prevents Nrf2 ubiquitination (Itoh et al., 2004). As a consequence, Nrf2 accumulates in nuclei, and after heterodimerization with Maf proteins, binds antioxidant response element (ARE)/electrophile response element (EpRE) and activates target genes for cytoprotection (Itoh et al., 2004). Due to its cytoprotective role, the Nrf2 increase in resistant cells has been proposed as an important tool for maintaining drug resistance (No et al, 2014). Indeed, Nrf2 overexpression is associated with clinically relevant CDDP resistance in bladder cancer patients (Hayden et al., 2014). Recently, in bladder cancer cells, we demonstrated a cross-talk between Nrf2 and Yap: Nrf2 silencing and glutathione depletion reduced YAP expression, possibly through the inhibition of GABP transcriptional activity (Ciamporcero et al., 2018). Moreover, YAP protein is also involved in maintaining antioxidant capacity: the stimulation of YAP prevents, whereas the down-regulation of YAP promotes oxidative stress-induced cell death in cardiomyocytes (Tao et al., 2016).

Increasing evidence has demonstrated the involvement of YAP in chemoresistance of several types of cancers. YAP, is a key component of the Hippo tumor-suppressor pathway (Harvey et al., 2013). Hippo pathway-mediated YAP phosphorylation on Ser127 leads to its cytoplasm sequestration or ubiquitination and degradation (Zhao et al., 2010). Conversely, unphosphorylated YAP translocates into the nucleus where it binds to the TEAD transcription factor, triggering the expression of several downstream transcriptional targets involved in organ size control, cell proliferation, migration and survival, such as c-Myc, cyr 61 and survivin. Indeed, YAP expression inhibition results in reduced

cell proliferation and increased cell death (Zhao et al., 2008). YAP expression and nuclear localization strongly correlate with poor patient outcome and the progression of several tumors, including bladder cancer (Liu et al., 2013). The constitutive expression and activation of YAP was inversely correlated with *in vitro* and *in vivo* CDDP sensitivity of urothelial cell carcinoma cells: YAP overexpression protects, while YAP knockdown sensitizes cancer cells to chemotherapy and radiation effects via increased accumulation of DNA damage and apoptosis (Ciamporcero et al., 2016). Moreover, the knockdown of YAP and the silencing of Nrf2 enhanced sensitivity of bladder cancer cells to CDDP and reduced their migration (Ciamporcero et al., 2018).
Aila has been demonstrated to exhibit in vitro growth-inhibitory effects against several cancer cell lines. However, the antitumor activity in bladder cancer cells, sensitive and resistant to CDDP treatment, remains to be elucidated. In this paper we demonstrated, for the first time, that Aila is able to inhibit proliferation and migration in these cell models, in particular in CDDP resistant cells, and that these effects could be linked to its ability to inhibit Nrf2, Yap and Myc expressions.

Materials and Methods

Cells and culture conditions

253J B-V and 253J cell lines were kindly provided by Dr Colin Dinney (MD Anderson Cancer Center). Human cell line T24 was purchased from ATCC (Manassas, VA, USA). These cells were cultured in RPMI 1640, supplemented with 10% FBS, 100 units per ml penicillin and 100μg/ml streptomycin in a 5% CO 2, 37°C incubator. The CDDP resistance in 253J B-V and 253J was induced and maintained as previously described (Ciamporcero et al., 2018).

MTT assay

The toxic effect of Aila was determined through the 3-(4,5-dimethyl thiazol-2-yl)-2,5-diphenyltetrazolium bromide (MTT) assay as previously described (Ciamporcero et al., 2018). This colorimetric assay may be interpreted as a measure of both cell viability and cell proliferation (Sylvester, 2011). Cells were seeded (800–1500 cells/well) in 200 μl of serum-supplemented medium and treated with different concentrations of Aila (Baoji Herbest Bio-Tech Co., Ltd., Baoji city Shannxi Provence China). To confirm the CDDP resistance, CDDP was added at the concentrations ranging from 0.1 to 1 μg/ml. Untreated cells were used as control. After 72 hours, the drug was removed and MTT assay was performed.

Colony-forming assay

Cells were trypsinized, washed in 1× PBS, and seeded (500 cells/well) into a six-well plate and left overnight to attach. After 24 h, the cells were treated with the compounds and the medium was changed after 72 h. Cells were cultured for 9–11 days and subsequently fixed and stained with a solution of 90% crystal violet (Sigma–Aldrich), 10% methanol.

Lysate preparation and western blot analysis

Lysate preparation and western blot analysis were performed as previously described (Ciampocero et al,, 2018). Antibodies used were as follows: glyceraldehyde 3 phosphate dehydrogenase (GAPDH) (#5174) (Cell Signaling, Boston, MA, USA); β-actin (sc-47778), YAP (sc15407), Nrf2 (sc 722), α-tubulin (04-1117, Millipore, Billerica, MA, USA); c-Myc (clone 9E10, sc 40, Santa Cruz Biotechnology, CA), GSTA4 (Glutathione S-transferase A4) (SAB1401164, Sigma–Aldrich). The detection of the bands was carried out after reaction with chemiluminescence reagents (PerkinElmer NEL105001EA) through film (Santa Cruz Biotechnology sc-201697) autoradiography.

Cytofluorimetric analysis

Adherent and non-adherent treated and control cells were harvested 24 hours after the treatment with 0.5 and 1 μg/ml of Aila. Cells were washed with 1X PBS, fixed in 70% cold ethanol, resuspended in a buffer containing 0.02 mg/ml RNase A (Worthington), 0.05 mg/ml propidium iodide (PI) (Sigma–Aldrich), 0.2% v/v Nonidet P-40 (Sigma–Aldrich), 0.1% w/v sodium citrate (Sigma–Aldrich), and analyzed with a FACScan cytometer (Becton Dickinson, Accuri). For apoptosis analysis $1x10^6$ cells were harvested and stained with FITC-Annexin 5 and PI according to the manufacter protocol (FITC Annexin V Apoptosis Detection Kit (BD Biosciences Cat N° 556547).

Cell motility assay

In the wound-healing assay, after starvation for 18–24 h in serum-free medium, cells were plated onto six-well plates (10^6 cell/well) and grown to confluence. Cell monolayers were wounded by scratching with a pipette tip along the diameter of the well, and they were washed twice with serum-free medium before their incubation with diverse concentrations of Aila (0.01, 0.05 and 0.1 μg/ml). In order to monitor cell movement into the wounded area, five fields of each wound were photographed immediately after the scratch (T0) and after 24 hours (Dianzani et al., 2014). The endpoint of the assay was measured by calculating the reduction in the width of the wound after 24 hours and compared to T0 which is set at 100%. The area of wound healing was calculated by using the ImageJ software (Schneider et al., 2012). In the Boyden chamber (BD Biosciences, San Jose, CA) invasion assay, cells (2000) were plated onto the apical side of 50 μg mL^{-1} Matrigel-coated filters (8.2 mm diameter and 0.5 μm pore size; Neuro Probe, Inc.; BIOMAP snc, Milan, Italy) in serum-free medium with or without increasing concentration of the Aila (0.01, 0.05 and 0.1 μg/ml). Medium containing 20% FCS was placed in the basolateral chamber as a chemo attractant. After 24 hours, cells on the apical side were wiped off with Q-tips. Cells on the bottom of the filter were stained with crystal violet and counted (five fields of each triplicate filter) with an inverted microscope.

Statistical analysis

Data were expressed as means ± SD. Significance between experimental groups was determined by one-way ANOVA followed by the Bonferroni multiple comparison post-test using GraphPad InStat software (San Diego, CA, USA). Values of $p \leq 0.05$ were considered statistically significant.

Results

Aila effect on bladder cancer cell growth and colony forming.

To analyze the ability of Alia to affect cell growth and colony forming of sensitive and CDDP-resistant bladder cancer cells, 253J B-V and 253J B-V resistant to CDDP (253J B-V C-r), 253J and 253J resistant to CDDP (253J C-r), and T24 (intrinsically CDDP resistant) cells were exposed to different doses of Aila. Results obtained demonstrated that the Alia was more effective than CDDP in reducing cell growth of 253J B-V cells and, in particular, Aila reduced the growth of 253J B-V C-r cells to the same extent as the sensitive cells (Fig. 1A). Colony forming assay confirmed the effectiveness of Aila treatment in sensitive and CDDP resistant 253J B-V cells (Fig. 1B).

The cytotoxic and antiproliferative effect of Aila was demonstrated in 253J cells, also (Fig. 2). The reduction of proliferation after 72 hours from the treatment with 0.5 and 1 μg/ml of Aila was similar in sensitive and CDDP resistant cells (Fig. 2A). The colony forming assay also confirmed the effectiveness of Aila in 253J C-r cells (Fig. 2B). The third cell line employed in our experiments was the T24 cells. This cell line has been demonstrated to be resistant not only to CDDP but also to other DNA damaging agents such as the anthracycline antibiotic doxorubicin and the Podophyllum peltatum toxin etoposide (Ciamporcero et al., 2016). Analogously, to that observed in the previous

cell lines, Aila reduced T24 cell growth and colony forming to a higher extent than CDDP (Fig.3 A, B).

Aila effects on Nrf2 and Nrf2 target gene expressions

We previously demonstrated that Nrf2 expression is higher in CDDP-resistant bladder cancer cells than in sensitive cells and that the silencing of Nrf2 in CDDP resistant bladder cancer cells, can sensitize them to CDDP and reduce cell viability (Ciamporcero et al., 2018). Since the Aila treatment reduced proliferation and colony forming of CDDP resistant cells to the same extent as the sensitive cells, we analyzed whether Aila could reduce Nrf2 expression in these cell lines. The analysis were performed after 24 and 48 hours from the treatment. Results demonstrated that Nrf2 expression was inhibited until 48 hours in a dose dependent way in both sensitive and resistant bladder cancer cells (Fig. 4 A,B). The reduction of Nrf2 protein was confirmed by the contemporary reduction of GSTA4, a Nrf2 target gene (Fig 5 A,B).

Effect of Aila on cell cycle and apoptosis of bladder cancer cells

To deepen the antiproliferative activity by Aila we performed the analysis of cell cycle and apoptosis in sensitive and CDDP-resistant 253J B-V cells. In both cell lines, Aila (from 0.1 to 1 μg/ml) induced a significant increase in G0/G1 cells (Fig. 6 A,B), whereas treatments with the same concentrations of Aila did not induce increase of apoptotic cells (data not shown).

Aila inhibits YAP and c-Myc protein expression

On the basis of our previous results that indicated a cross-talk between Nrf2 and YAP expression, we analyzed in 253J B-V and 253J B-V C-r the expression of YAP. Moreover, since Myc and YAP-TEAD integrate mitogenic and mechanical cues at the transcriptional level to control cell proliferation (Croci et al., 2017), c-Myc protein expression was also examined. Results obtained demonstrated that Aila inhibited YAP and c-Myc expression, both in sensitive and, particularly, in resistant cell lines, which express YAP at high levels (Fig.7 A,B). The inhibition was dose-dependent and persisted until 48 hours from the treatment.

Effects of Aila on migration of bladder cancer cells

YAP and Nrf2 also control the migration of cancer cells (Rojo de la Vega et al., 2018) which contributes to their metastatic properties. Since Aila inhibited the expression of both Nrf2 and YAP proteins, we analyzed its effect on cell migration. Cell motility was initially assessed using a wound healing assay evaluating random cell migration in the presence or absence of diverse concentrations of Aila (from 0.01 to 0.1 μg/ml). Analysis of the cell ability to migrate into the scratch showed that Aila inhibited migration of both cell lines (Fig. 8 A,B) in a dose-dependent way. However, the effect in CDDP-resistant cells was higher than in sensitive cells. Then, cell motility was assessed using a Boyden chamber assay assessing directional migration and invasion of cells. Results showed that Aila inhibited 253J B-V and 253J B-V C-r cell invasion in a concentration dependent way in both cell lines, but, interestingly, the invasion of the CDDP-resistant cells was affected at higher levels than the sensitive cells (Fig. 9). Control invasion was 72±5 cells per wells for 253J B-V and 84±4 for 253J B-V C-r. Data are shown as percentages of inhibition versus the control invasion measured on untreated cells. In both migration assays, doses and timing of treatments minimized the possible confounding effects due to the Aila effect on cell growth.

Discussion

In the present study, Aila was found to be able to inhibit the proliferation of sensitive and CDDP resistant bladder cancer cells with the same effectiveness. The inhibition of proliferation mostly depended on the accumulation of cells in G0/G1 cell cycle phase of cell cycle, which, in turn, could be dependent on the Nrf2, Yap and c-Myc down-regulation. Nrf2 and YAP expression are increased

in resistant cells (Ciamporcero et al, 2016; Ciamporcero et al., 2018) and both play an important role in reducing proliferative capacity of cells. Beside the canonical Nrf2 role in orchestrating antioxidant response, accumulating evidence has established that Nrf2 sustained proliferative signaling and that its reduction correlated with a reduction of cell proliferation (Rojo de la Vega et al., 2018). As a consequence, the down regulation of Nrf2 expression by Aila, could reduce the cytoprotective role of Nrf2, thus facilitating its own antiproliferative action. Another naturally occurring quassonoid, brusatol, extracted from the aerial parts of the *Brucea javanica* plant, has been shown to inhibit Nrf2 and to sensitize cancer cells to several chemotherapeutic drugs (Ren et al., 2011). However, the brusatol-mediated inhibition of Nrf2 was transient, persisting only 8 hours from the treatment (Olayanju A et al., 2015). On the contrary, we demonstrated that after 48 hours the reduction of Nrf2 expression by Aila was still present, as well as the reduction of the Nrf2 target gene GSTA4. The high antiproliferative effect of Aila in CDDP-resistant cells could be sustained not only by this persistent inhibition of Nrf2 expression, but also by the contemporary inhibition of YAP and Myc expression. Indeed YAP, through the activation of TEAD transcription factors, has been demonstrated to be implicated in the control of growth, oncogenic transformation, and epithelial-mesenchymal transition (Zao et al, 2008). Moreover, the binding of YAP with TEADs upregulates the expression of several growth promoting factors, among those is the well known oncogene c-myc (Neto- Silva et al., 2010). C-Myc and YAP-TEAD integrate mitogenic and mechanical cues at the transcriptional level to control cell proliferation and cell cycle entry (Croci et al., 2017).

Traditionally, the cytotoxic effect of platinum compounds depend on the formation of intrastrand DNA cross-links [mostly double-strand breaks (DSB)], that lead to G2 arrest, apoptosis induction and generation of oxidative stress (Yu et al., 2018). In this study we demonstrated that Aila affected cell growth through mechanisms other than cisplatin. In our cell models, Aila induced a cell cycle arrest in G0/G1 cells which can be in relation with the inhibition of YAP and c-Myc expression. Moreover, no evidence of apoptosis induction was present, even after the treatment with the highest Aila concentration. Thus, apoptosis seems not be involved in the reduction of cell growth.

Another important effect displayed by low doses of Aila regarded the inhibition of both random and directional migration. In determining this inhibitory effect, different pathways can be involved, in which both Nrf2 and YAP play an important role (Zhang et al., 2016; Warren et al., 2018).

In cancer cell lines, Nrf2 promoted the epithelial mesenchimal transition by down-regulation of E-caderin, and Nrf2 knock-down greatly impaired migration and invasion (Rojo de la Vega et al., 2018). For its part, YAP also is involved in cell invasion, since it induced epithelial mesenchimal transition in cancer cells and YAP knock-down rescued the expression of epithelial markers (Zhao et al., 2008).

Conclusions

Our results demonstrated, for the first time, that Aila inhibited proliferation and migration of bladder cancer cells, by reducing Nrf2, YAP and c-Myc expression. Importantly, this effect was displayed in CDDP-resistant cancer cells in which the down-regulation of Nrf2 and YAP expressions was required to overcome the resistance. Since CDDP resistance is a common feature in muscle invasive urothelial carcinoma of the bladder after platinum-based chemotherapy (Shah et al., 2011), the identification of a novel agent able to overcome this resistant disease is of great interest. From this point of view, Aila demonstrated favourable drug-like properties due to its good bioavailability, high solubility and low hepatoxicity (He et al, 2015).

In conclusion our results suggest that Aila may represent an important tool in the therapy of CDDP-resistant bladder cancer and pave the way for further investigation in this field.

Acknowledgments: This work was supported by the University of Torino " Ricerca Locale "ex 60%" Department of Clinical and Biological Sciences (BARG-RILO-16-01 and PIZS-RILO- 17-01), Ricerca Locale "ex 60%" Department of Sciences and Pharmaceutical Technology (DIAC-RILO-16-01 and DIAC-RILO-17-01), and CRT 2016 (TROFCRT1602).

Conflict of interest

The authors declare no conflict of interest.

References

Bray, D.H., Boardman, P., O'Neill, M.J., Chan, K.L., Phillipson, J.D., Warhurst, D.C., Suffness, M., 1987. Plants as a source of antimalarial drugs 5. Activities of Ailanthus altissima stem constituents and of some related quassinoids. Phytother. Res. 1, 22–24.

Chen, Y., Zhu, L., Yang, X., Wei, C., Chen, C., He, Y., Ji, Z., 2017. Ailanthone induces G2/M cell cycle arrest and apoptosis of SGC-7901 human gastric cancer cells. Mol Med Rep. 16, 6821-6827.

Ciamporcero, E., Shen , H., Ramakrishnan, S., Yu Ku, S., Chintala, S., Shen, L., Adelaiye, R., Miles, K.M., Ullio, C., Pizzimenti, S., Daga, M., Azabdaftari, G., Attwood, K., Johnson, C., Zhang, J., Barrera, G., Pili, R., 2016. YAP activation protects urothelial cell carcinoma from treatment-induced DNA damage. Oncogene. 35, 1541-1553.

Ciamporcero, E., Daga, M., Pizzimenti, S., Roetto, A., Dianzani, C., Compagnone, A., Palmieri ,A., Ullio, C., Cangemi, L., Pili, R., Barrera, G., 2018. Crosstalk between Nrf2 and YAP contributes to maintaining the antioxidant potential and chemoresistance in bladder cancer. Free Radic Biol Med. 115, 447-457.

Croci, O., De Fazio, S., Biagioni, F., Donato, E., Caganova, M., Curti, L., Doni, M., Sberna, S., Aldeghi, D., Biancotto, C., Verrecchia, A., Olivero, D., Amati, B., Campaner, S., 2017. Transcriptional integration of mitogenic and mechanical signals by Myc and YAP. Genes Dev. 31, 2017-2022.

Dianzani, C., Minelli, R., Gigliotti, C.L., Occhipinti, S., Giovarelli, M., Conti, L., Boggio, E., Shivakumar, Y., Baldanzi, G., Malacarne, V., Orilieri, E., Cappellano, G., Fantozzi, R., Sblattero, D., Yagi, J., Rojo, J.M., Chiocchetti, A., Dianzani, U., 2014. B7h triggering inhibits the migration of tumor cell lines. J Immunol. 192, 4921-4931.

Harvey, K.F., Zhang, X., Thomas, D.M., 2013. The Hippo pathway and human cancer. Nat Rev Cancer 13, 246–257.

Hayden, A., Douglas, J., Sommerlad, M., Andrews, L., Gould, K., Hussain, S., Thomas, G.J., Packham, G., Crabb, S.J., 2014. The Nrf2 transcription factor contributes to resistance to cisplatin in bladder cancer. Urol Oncol. 32, 806-814.

He, Y., Peng, S., Wang, J., Chen, H., Cong, X., Chen, A., Hu, M., Qin, M., Wu, H., Gao, S., Wang, L., Wang, X., Yi, Z., Liu, M., 2016. Ailanthone targets p23 to overcome MDV3100 resistance in castration-resistant prostate cancer. Nat Commun. 7, 13122. http://doi.org/10.1038/ncomms13122

Itoh, K.,Tong, KI., Yamamoto, M., 2004. Molecular mechanism activating Nrf2-Keap1 pathway in regulation of adaptive response to electrophiles. Free Radic Biol Med. 36, 1208–1213.

Kim, H.M., Kim, S.J., Kim, H.Y., Ryu, B., Kwak, H., Hur, J., Choi, J.H., Jang, D.S., 2015. Constituents of the stem barks of Ailanthus altissima and their potential to inhibit LPS-induced nitric oxide production. Pharm Biol. 54, 1641–1648.

Liu, J.Y., Li, Y.H., Lin, H.X., Liao, Y.J., Mai, S.J., Liu, Z.W., Zhang, Z.L., Jiang, L.J., Zhang, J.X., Kung, H.F., Zeng, Y.X., Zhou, F.J., Xie, D., 2013. Overexpression of YAP 1 contributes to progressive features and poor prognosis of human urothelial carcinoma of the bladder. BMC Cancer. 13,349. http://doi.org/10.1186/1471-2407-13-349

Madersbacher, S., Hochreiter ,W., Burkhard, F., Thalmann, G.N., Danuser, H., Markwalder, R., Studer, U.E., 2003. Radical cystectomy for bladder cancer today–a homogeneous series without neoadjuvant therapy. J Clin Oncol. 21, 690–696.

Neto-Silva, R.M., de Beco, S., Johnston, L.A., 2010. Evidence for a growth-stabilizing regulatory feedback mechanism between Myc and Yorkie, the Drosophila homolog of Yap. Dev Cell. 19, 507–520.

Ni, Z., Yao, C., Zhu, X., Gong, C., Xu, Z., Wang, L., Li, S., Zou, C., Zhu, S., 2017. Ailanthone inhibits non-small cell lung cancer cell growth through repressing DNA replication via downregulating RPA1. Br J Cancer. 117, 1621-1630.

No, J.H., Kim, Y.B., Song, Y.S., 2014. Targeting nrf2 signaling to combat chemoresistance. J Cancer Prev.19, 111-117.

Olayanju, A., Copple, I.M., Bryan, H.K., Edge, G.T., Sison, R.L., Wong, M.W., Lai, Z.Q., Lin, Z.X., Dunn, K., Sanderson, C.M., Alghanem, A.F., Cross, M.J., Ellis, E.C., Ingelman-Sundberg, M., malik, H.Z., Kitteringham N.R., Goldring, C.E., Park, B.K., 2015. Brusatol provokes a rapid and transient inhibition of Nrf2 signaling and sensitizes mammalian cells to chemical toxicity-implications for therapeutic targeting of Nrf2. Free Radic Biol Med. 78, 202–212.

Ren, D., Villeneuve, N.F., Jiang, T., Wu, T., Lau, A., Toppin, H.A., Zhang, D.D., 2011. Brusatol enhances the efficacy of chemotherapy by inhibiting the Nrf2-mediated defense mechanism. Proc Natl Acad Sci U S A. 108, 1433–1438.

Rojo de la Vega, M., Chapman, E., Zhang, D.D., 2018. NRF2 and the Hallmarks of Cancer. Cancer Cell. pii: S1535-6108(18)30127-2. https://doi.org/10.1016/j.ccell.2018.03.022

Schneider, C.A., Rasband, W.S., Eliceiri, K.W., 2012. NIH Image to ImageJ: 25 years of image analysis Nat. Methods 9, 671-675.

Shah, J.B., McConkey, D.J., Dinney, C.P., 2011. New strategies in muscle-invasive bladder cancer: on the road to personalized medicine. Clin Cancer Res. 17, 2608–2612.

Sylvester , P.W., 2011. Optimization of the tetrazolium dye (MTT) colorimetric assay for cellular growth and viability. Methods Mol. Biol., 716, 157-168.

Tao, G., Kahr, P.C., Morikawa, Y., Zhang, M., Rahmani, M., Heallen, T.R., Li, L., Sun, Z., Olson, E.N., Amendt, B.A., Martin, J.F., 2016. Pitx2 promotes heart repair by activating the antioxidant response after cardiac injury. Nature. 534, 119-123.

Wang, R., Xu, Q., Liu, L., Liang, X., Cheng, L., Zhang, M., Shi, Q., 2016. Antitumour activity of 2-dihydroailanthone from the bark of Ailanthus altissima against U251. Pharm Biol. 54, 1641–1648.

Warren, J.S.A., Xiao, Y., Lamar, J.M., 2018. YAP/TAZ Activation as a Target for Treating Metastatic Cancer. Cancers (Basel). 10(4), pii: E115. http://doi.org/10.3390/cancers10040115

Yu, W., Chen, Y., Dubrulle, J., Stossi, F., Putluri, V., Sreekumar, A., Putluri, N., Baluya, D., Lai, S.Y., Sandulache ,V.C., 2018. Cisplatin generates oxidative stress which is accompanied by rapid shifts in central carbon metabolism. Sci Rep. 8(1),4306**.** http://doi.org/10.1038/s41598-018-22640-y

Zhang, C., Wang, H.J., Bao, Q.C., Wang, L., Guo, T.K., Chen, W.L., Xu, L.L., Zhou, H.S., Bian, J.L., Yang,YR., Sun, H.P., Xu, X.L., You, Q.D., 2016. NRF2 promotes breast cancer cell proliferation and metastasis by increasing RhoA/ROCK pathway signal transduction. Oncotarget. 7, 73593-73606.

Zhao, B., Ye, X., Yu, J., Li, L., Li, W., Li, S., Yu, J., Lin, J.D., Wang, C.Y., Chinnaiyan, A.M., Lai, Z.C., Guan, K.L., 2008. TEAD mediates YAP-dependent gene induction and growth control. Genes Dev. 22, 1962–1971.

Zhao, B., Li, L., Tumaneng, K., Wang, C.Y., Guan, K.L., 2010. A coordinated phosphorylation by Lats and CK1 regulates YAP stability through SCF (beta-TRCP). Genes Dev. 24, 72–85.

Zhuo, Z., Hu, J., Yang, X., Chen, M., Lei, X., Deng, L., Yao, N., Peng, Q., Chen, Z., Ye, W., Zhang, D., 2015. Ailanthone Inhibits Huh7 Cancer Cell Growth via Cell Cycle Arrest and Apoptosis In Vitro and In Vivo. Sci Rep. 5,16185. http://doi.org/10.1038/srep16185

Figure legends

Figure 1. MTT and colony forming assays in 253J B-V and 253J BV C-r cells. **Panel A**: MTT assay. Results are expressed as percent of control values, obtained after 72 hours from the treatment with the indicated concentrations of Aila or CDDP. Results are the mean ± SD of four separate experiments. **p≤0.01vs sensitive cells. **Panel B**: Colony forming assay. Cells were treated with the indicated concentrations of Aila or CDDP and cultured for 10 days.

Figure 2. MTT and colony forming assays in 253J and 253J C-r cells. **Panel A**: MTT assay. Results are expressed as percent of control values, obtained after 72 hours from the treatment with the indicated concentrations of Aila or CDDP. Results are the mean ± SD of four separate experiments. **p≤0.01vs sensitive cells. **Panel B**: Colony forming assay. Cells were treated with the indicated concentrations of Aila or CDDP and cultured for 10 days.

Figure 3. MTT and colony forming assays in T24 cells. **Panel A**: MTT assay. Results are expressed as percent of control values, obtained after 72 hours from the treatment with the indicated concentrations of Aila or CDDP. Results are the mean ± SD of four separate experiments. **Panel B**: Colony forming assay. Cells were treated with the indicated concentrations of Aila or CDDP and cultured for 10 days.

Figure 4. **Panel A**: Western blot analysis of Nrf2, expression in 253J B-V , 253J BV C-r, 253J, 253J C-r and T24 cells in untreated (0) or treated with Aila at the indicated concentrations and harvested after 24 or 48 hours. Equal protein loading was confirmed by exposure of the membranes

to the anti-β-actin antibody. Quantification of protein products was performed by densitometric scanning. Data are normalized using the β-actin signal and are indicated as means ± SD from three independent experiments. **Panel B**: Quantification of protein products was performed by densitometric scanning. Data were normalized using the β -actin signal and are indicated as the mean ± SD from three independent experiments. ** p-value ≤0.01 vs. untreated control cells (C).

Figure 5. **Panel A**: Western blot analysis of GSTA4 expression in 253J B-V, 253 J B-V C-r , 253J, 253J C-r and T24, untreated (0) or treated with Aila at the indicated concentrations and harvested after 48h. Equal protein loading was confirmed by exposure of the membranes to the anti-α-tubulin antibody. **Panel B**: Quantification of protein products was performed by densitometric scanning. Data were normalized using the α-tubulin signal and are indicated as the mean ± SD from three independent experiments. ** p-value ≤0.01 and * p-value ≤0.05 vs. untreated control cells (C).

Figure 6. **Panel A**: Cell-cycle analysis in untreated (Control, C) or treated with 0.1 μg/ml Aila (0.1 Aila) or with 0.5 μg/ml Aila (0.5 Aila) in 253J B-V and 253 J B-V C-r , at 24 hours. The data were captured by using a BD Accuri Flow cytometer. Results were extracted and analysed by using FCS Express Plus. Representative images and the relative percentages are shown. **Panel B**: Percent of cell in cell cycle phases 24 hours after treatment with 0.1 μg/ml Aila or 0.5 μg/ml Aila in 253J B-V and 253J B-V C-r. Data are the mean ± SD of 3 separate experiments. **p≤0.01, *p≤0.05 vs C.

Figure 7. **Panel A**: Western blot analysis of YAP and c-Myc expression in 253J B-V and 253J B-V C-r cells untreated (0) or treated with Aila at the indicated concentrations and harvested after 24h and 48 hours. Equal protein loading was confirmed by exposure of the membranes to the anti-β-actin antibody. **Panel B**: Quantification of protein products was performed by densitometric scanning. Data were normalized using the β -actin signal and are indicated as the mean ± SD from three independent experiments. ** p-value ≤0.01 vs. untreated control cells (C).

Figure 8. **Panel A**: wound healing assay at 0 (T0) and at 24 hours in 253J B-V and 253J B-V C-r cells untreated (C) or treated with Aila at the indicated concentrations. **Panel B**: Quantification of wound healing. The endpoint of the assay was measured by calculating the reduction in the width of the wound after 24 hours and compared to T0 which is set at 100%. The data of each assay was done from 3 independent experiments and shown as the mean ± SD. **p-value≤0.01 and *p≤0.05 vs. C.

Figure 9. Invasion assay at 24 hours in 253J B-V and 253J B-V C-r cells treated with Aila at the indicated concentrations. Data are expressed as percentages of inhibition of cell invasion versus the control invasion measured on untreated cells. The data of each assay was done from 5 independent experiments and shown as the mean ± SD. **p-value≤0.01 and *p≤0.05 vs. C.

Figure 1

Click here to download high resolution image

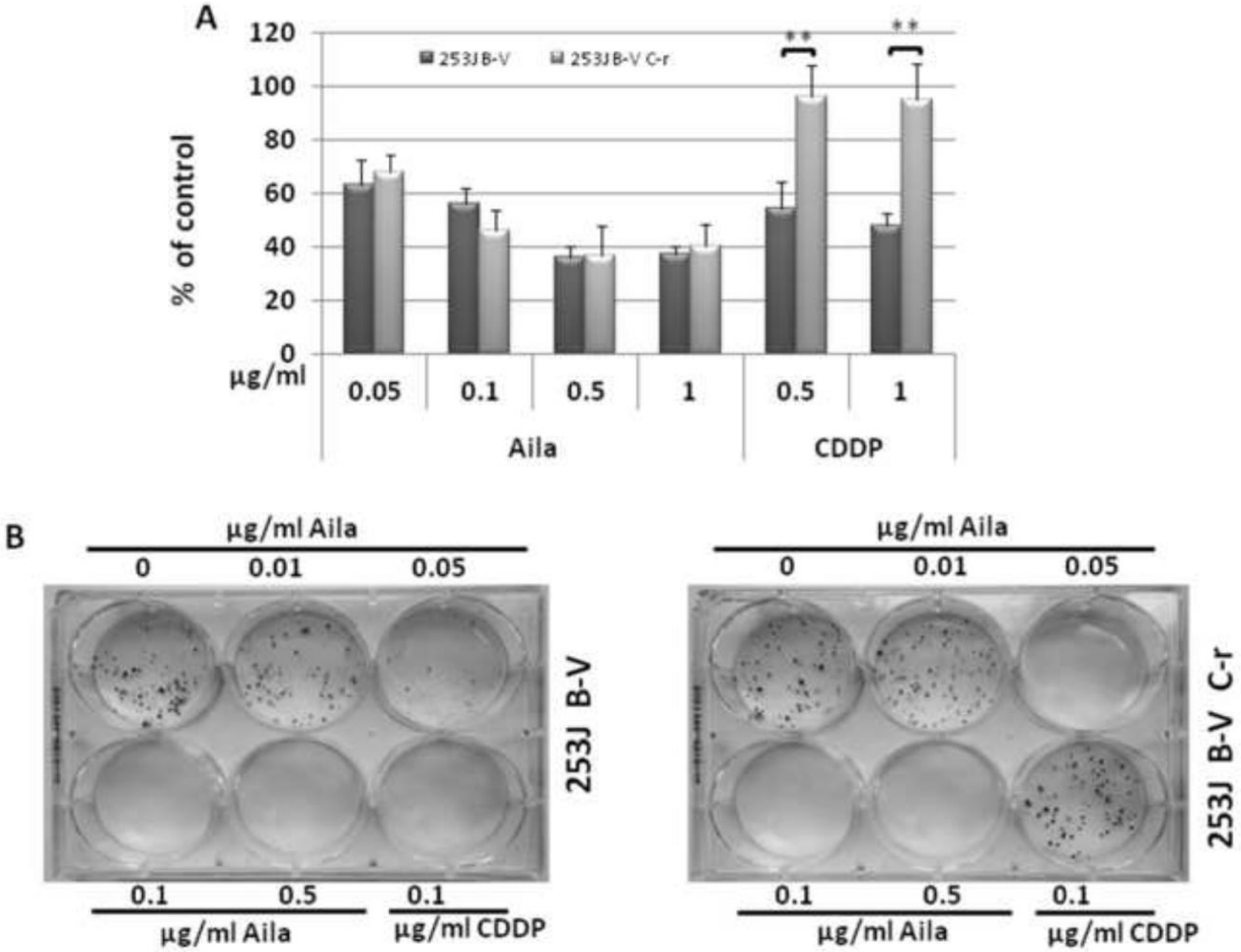

Figure 2

Click here to download high resolution image

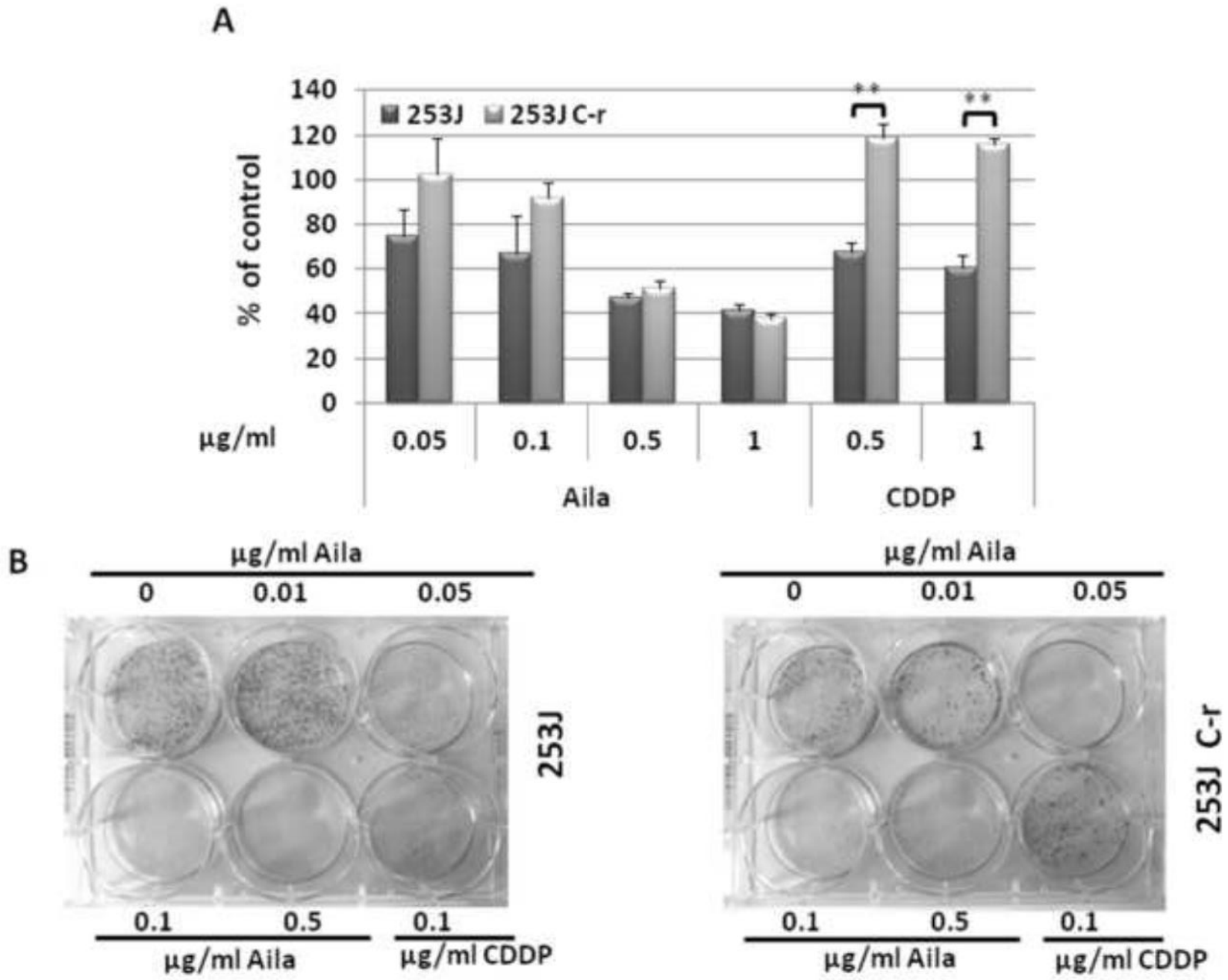

Figure 3
Click here to download high resolution image

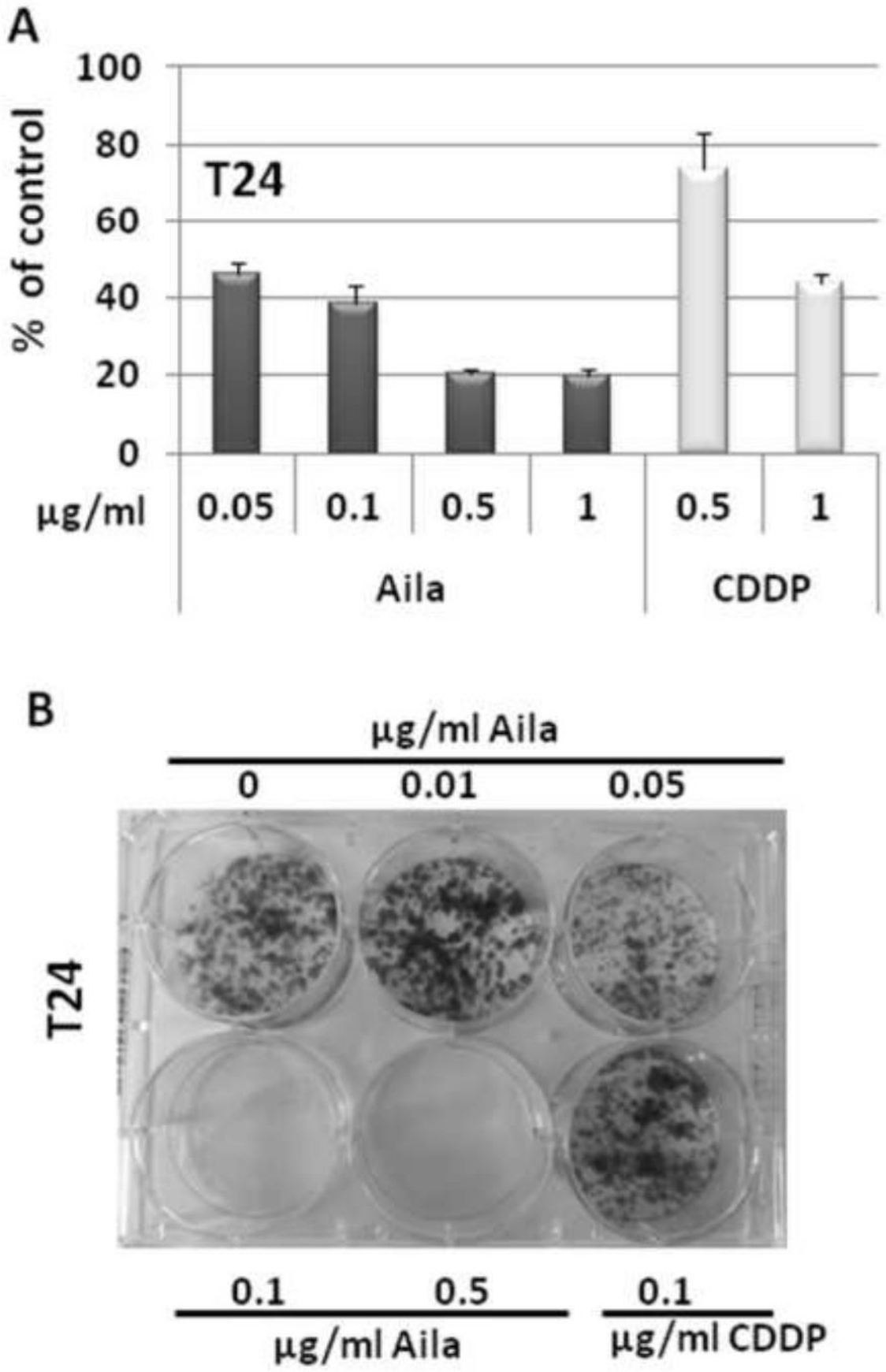

Figure 4

Click here to download high resolution image

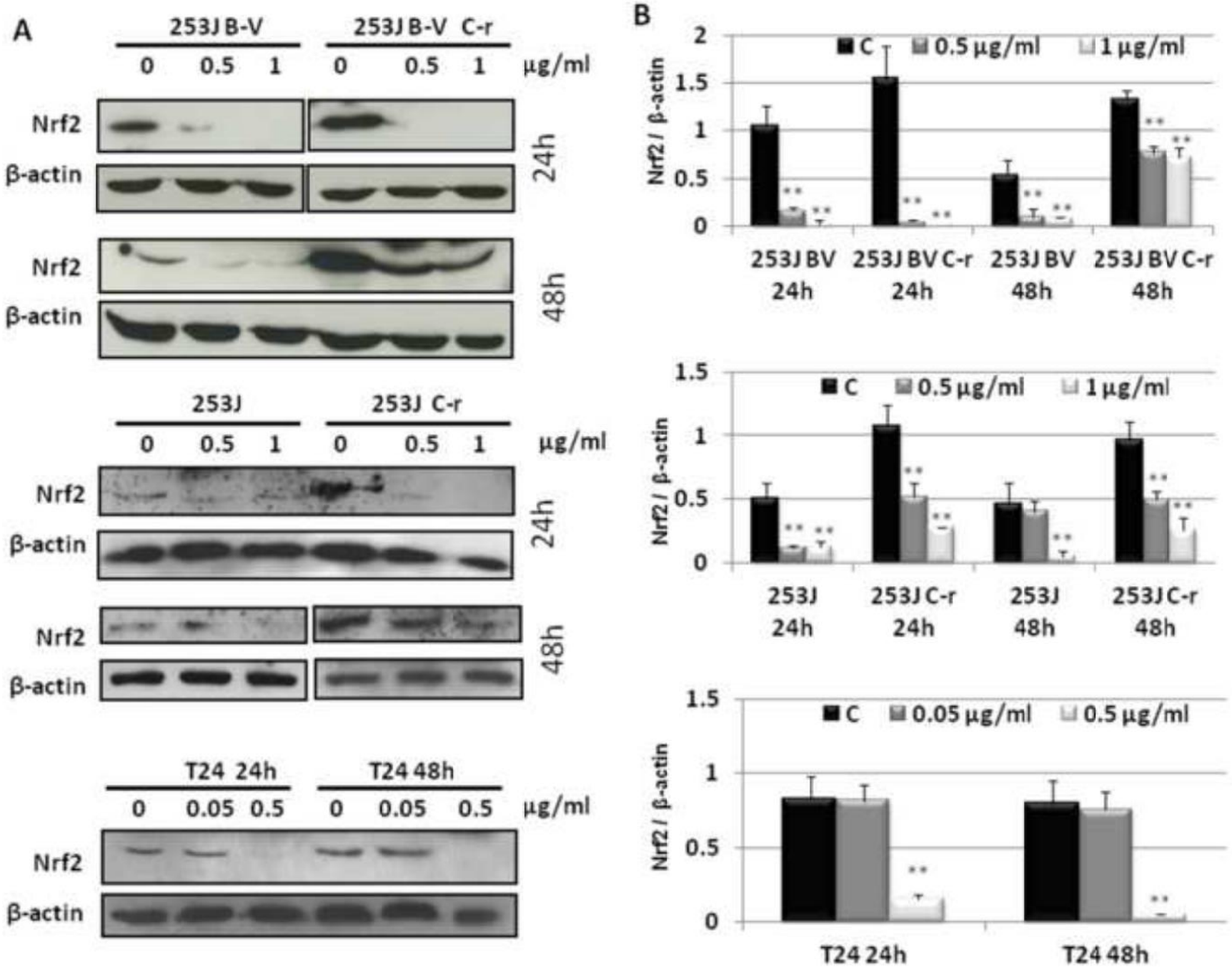

Figure 5

Click here to download high resolution image

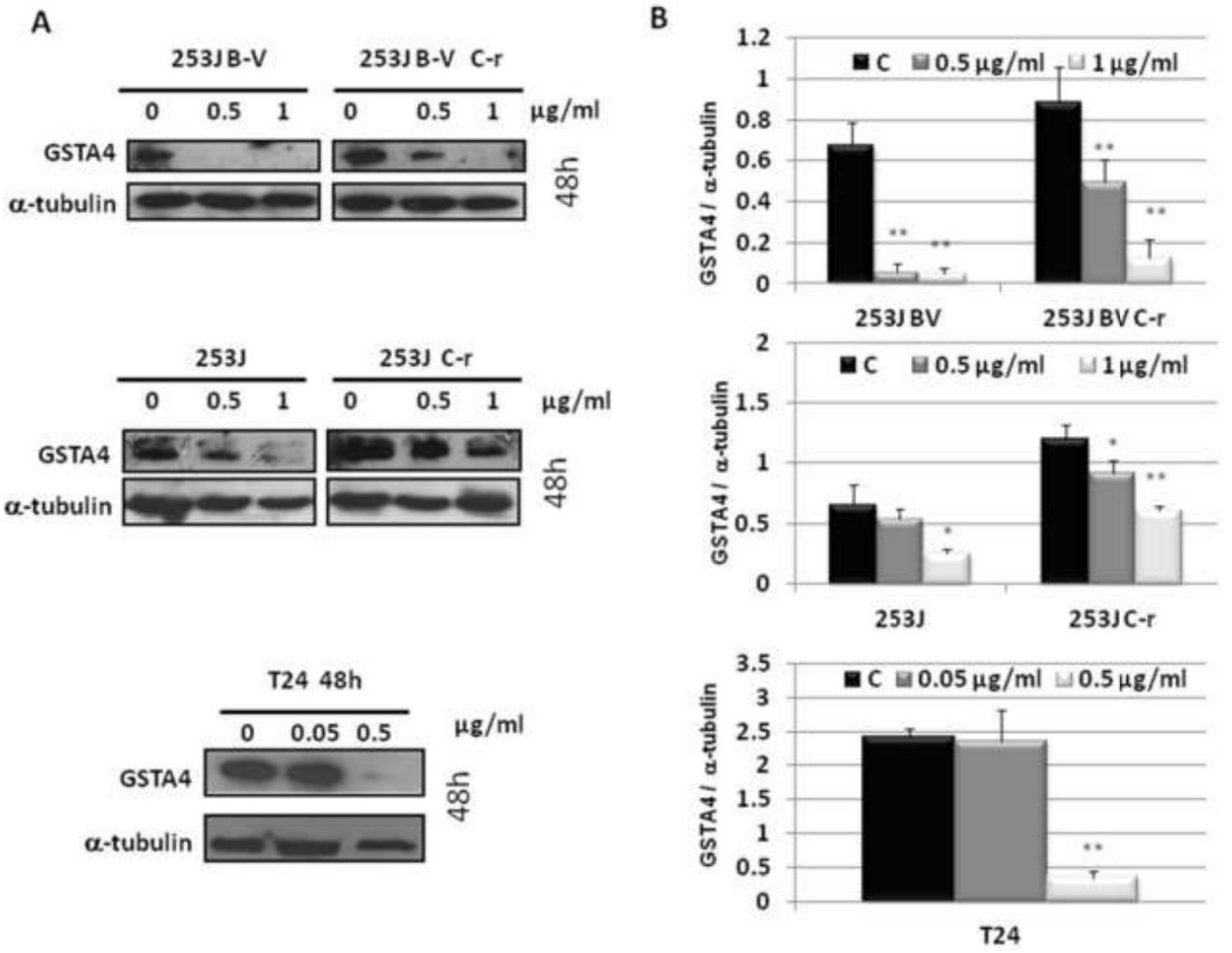

Figure 6

Click here to download high resolution image

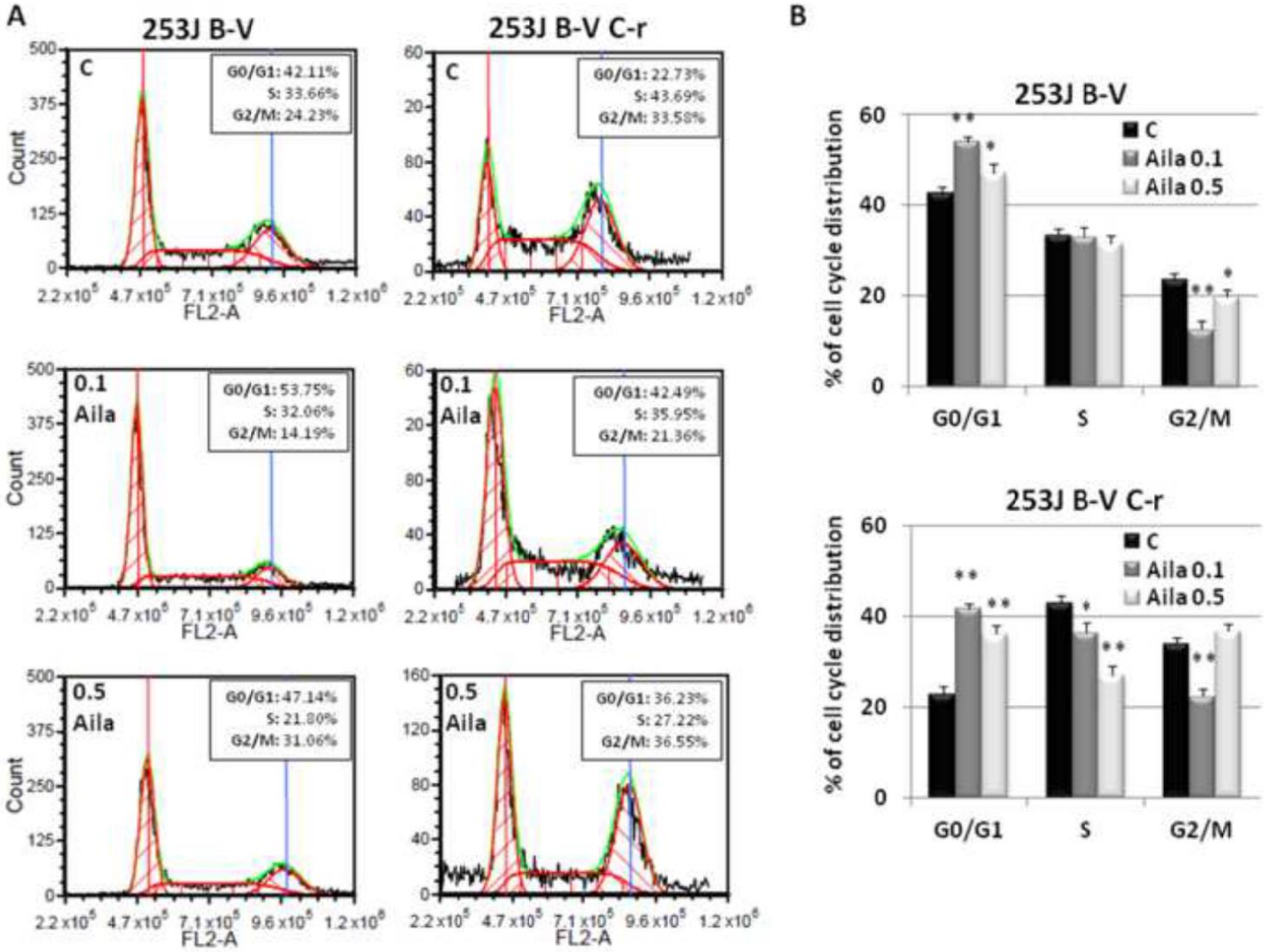

Figure 7

Click here to download high resolution image

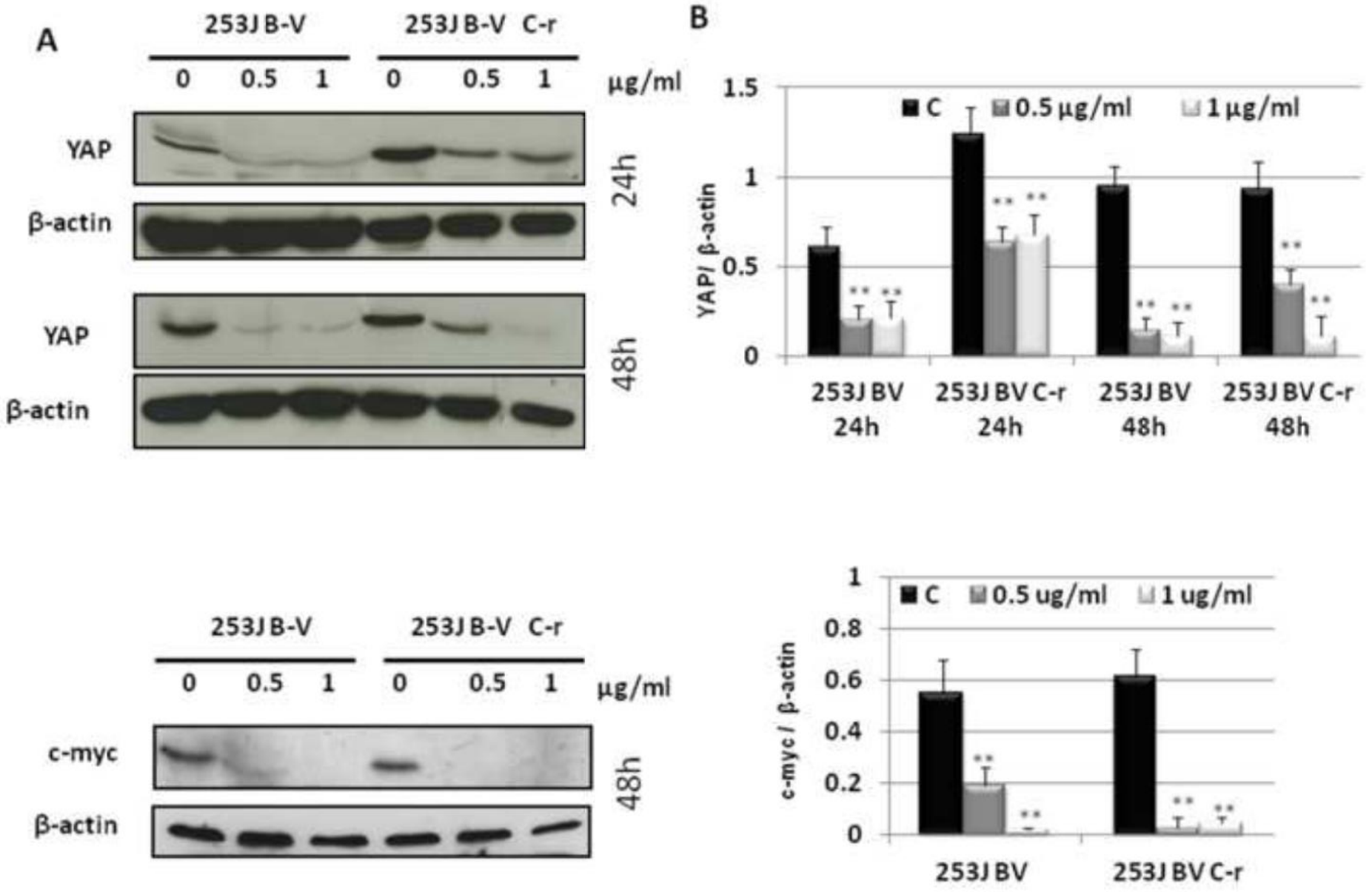

Figure 8

Click here to download high resolution image

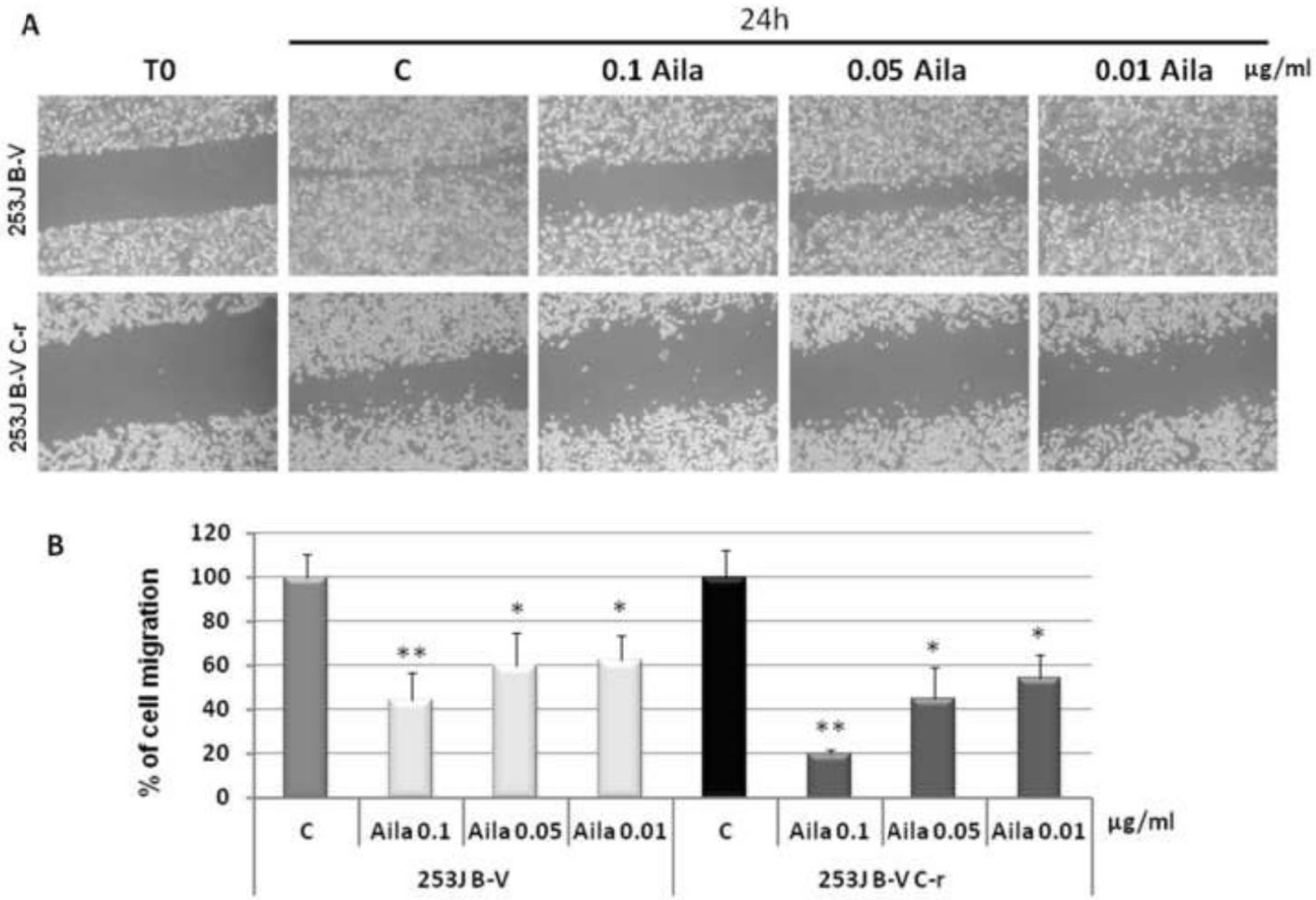

Figure 9

Click here to download high resolution image